DISCHARGE ESTIMATION FOR THE INVISIBLE AMAZON RIVER BRANCHES IN SAR IMAGES

Kyoichiro Katabira [a], Susumu Ogawa [b], Takako Sakurai [c], Mikio Takagi [d]

[a] Center for Spatial Information Science, University of Tokyo, 4-6-1 Komaba, Meguro-ku, Tokyo, 153-8505, Japan
katabira@iis.u-tokyo.ac.jp
[b] Faculty of Geo-Environment Science, Rissho University, 1700 Magechi, Kumagaya, Saitama, 360-0194, Japan
ogawa@ris.ac.jp
[c] Department of Applied Electronics, Science University of Tokyo - takako@rs.iis.u-tokyo.ac.jp
[d] Graduate School of Engineering, Shibaura Institute of Technology - mikio@sic.shibaura-it.ac.jp

KEY WORDS: Forestry, Geomorphology, Monitoring, Visualization, SAR

ABSTRACT:

Recently, desertification and degradation of water cycle by deforestation in the Amazon, South America, have become a serious problem. In this study, it was attempted to estimate the discharge of the invisible Amazon River branches in the JERS-1/SAR images for the purposes of the periodical environment and disaster monitoring. First, by SFP filters for SAR images, some traces of the very narrow open-water channels were visualized, which were not found in the original SAR images because of the resolution with less than 20 m. Next, the river shapes were transformed into one-dimensional signals, and the spatial frequencies were calculated with the Fourier and wavelet analyses. Furthermore, with river geomorphology or the Hack's and Horton's rules, the characteristics of the river shapes such as the meandering wavelength, the amplitude, the branch length and the number of branches were extracted from the SAR images. Then, It was compared that the characteristics of the river shapes with the existing discharge data and derived some regression equations. Finally, the discharge of the Amazon River branches was estimated from the SAR images.

1. INTRODUCTION

Recently, desertification and degradation of water cycle by deforestation in the Amazon, South America, have become a serious problem. In this study, we attempted to estimate the discharge of the Amazon River branches from JERS-1/SAR images, which are independent of the weather. According to the river geomorphology, the river shapes such as the amplitude and the meandering are related with its discharges. For example, a small meandering wavelength shows low discharge, while a big one shows high discharge. First, we visualized some traces of the Amazon River branches by filtering, which were not found in the original SAR images. Next, we transformed river shapes into a one-dimensional signal, and calculated the river characteristics or the spatial frequencies with the Fourier and wavelet analysis. These characteristics mean the average of the spatial frequencies of the river shapes, the angle of the meandering, the number of branches, the river slope, the river length, and the drainage area. Then, we related the characteristics of the river shapes with the existing discharge data and derived some regression equations. Finally, we estimated the discharge of the Amazon River branches from the SAR images.

2. METHOD

2.1 Study Area

We selected 11 stations in the Amazon Basin, and 12 scenes of JERS-1/SAR, which observed mostly rainy seasons from 1993 to 1997 at the near sites of the discharge measurement stations. Beside, we used the discharge data of the Amazon River branches, Rio Madeira, Rio Jipanara, Rio Purus, Rio Guapore, Rio Tabajara, and Rio Juruena, which were observed from 1965 to 1997. In the absence of discharge data on the same date of SAR observation, we used the mean discharge during the observation periods.

2.2 Approach to Estimate the River Discharges

First, to remove speckle noises in the original SAR images, we used a SFP filter and an enhanced SFP filter (1), and integrated two images. These filters could remove speckle noises while the small features were preserved.

Next, we emphasized the pixel value differences of the surroundings in order to extract the very thin rivers from the bright characteristic spots. The very narrow open-water channels did not show the dark characteristics, but intermittently showed the bright characteristics with the corner reflected effect. We prepared a 5-by-5 window, and calculated the sum of the absolute differences between a center pixel and its surrounding pixel values (2). Then, we emphasized the isolated string scatters, and visualized very thin rivers, which were not found in the original SAR images (Fig. 1).

$$x_c = \frac{\sum_{k=-m}^{m}\sum_{l=-n}^{n} w_{kl} z_{kl}}{\sum_{k=-m}^{m}\sum_{l=-n}^{n} w_{kl}} \qquad (1)$$

$$w_{kl} = \begin{cases} 1 & \text{if } |z_c - z_{kl}| < 2\sigma_v \overline{z_c} \\ 0 & \text{otherwise} \end{cases}$$

$$\sigma_v = 0.2536$$

$$x_c = \sum_{k=-m}^{m} \sum_{l=-n}^{n} \left| z_c - z_{kl} \right| \qquad (2)$$

where Z_c = a center pixel value in the window
Z_{kl} = a pixel value except the center
x_c = a center pixel value after filtering

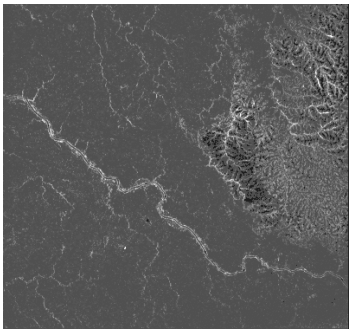

Fig. 1. Filtered SAR image (Path =416, Row =315, Tabajara)

Next, to extract the only river shapes, we applied binarizing and thinning for the images (Fig. 2). First, we obtained the coordinates through the river path at every constant interval, and calculated each angle from the adjacent line segment (Fig. 3). We determined this constant length was 20 pixels (500 m) because the smallest river wavelength was approximately 500 m. By this technique, we transformed the river shapes into a one-dimensional signal (Fig. 4). This signal showed that a small meandering had high frequency and big amplitude, while a large meandering had low frequency and small amplitude.

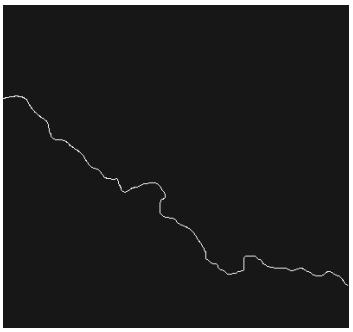

Fig. 2. Binarized image (Path =416, Row =315)

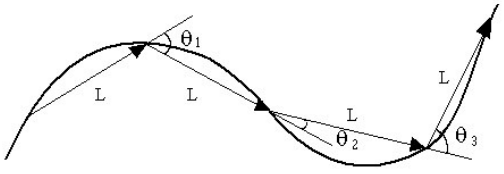

Fig. 3. Method of one-dimensional transformation

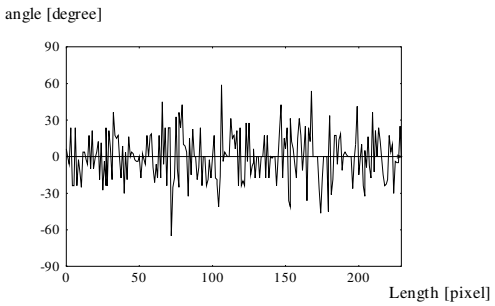

Fig. 4. One-dimensional signal (Path = 416, Row = 315)

Next, to analyze the spatial frequencies or the characteristics of the river shapes, we applied the Fourier and continuous wavelet transforms for the one-dimensional signals. In this technique, we could treat the river shapes in the spatial frequency domain. The mother wavelet that we applied was the Gabor wavelet expressed as the equation (3), which showed the best fitting wave for the original wave (Fig. 5). The wavelet's scale was equivalent to the frequency, and then the bigger scale was equivalent to the lower frequency. We show the space-frequency two-dimensional plane where an x axis corresponds to the spatial scale, a y axis corresponds to the wavelet's scale, and a z axis corresponds to the spectral intensity (Figs. 6 to 9).

$$W(b,a) = \frac{1}{\sqrt{a}} \int_R f(x) \overline{\psi\left(\frac{x-b}{a} \right)} dx$$
$$\psi(x) = \frac{1}{2\sqrt{\pi}\sigma} \exp\left(-\frac{x^2}{\sigma^2} \right) \exp(ix) \qquad (3)$$

where $W(b,a)$ = spectrum intensity
$f(x)$ = original signal
$\psi(x)$ = mother wavelet
a = scale
b = position

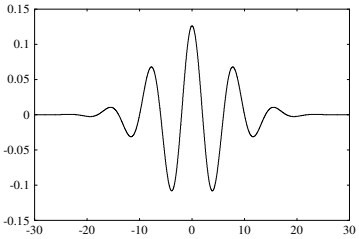

Fig. 5. Real part of Gobor wavelet

Moreover, we applied the multi-resolution analysis with a discrete wavelet transform to the original signals. In this technique, we analyzed which level of that frequency was included in which part of the signals. The level corresponded to the frequency, and then the higher level was equivalent to

the lower frequency. This mother wavelet that we applied was the Daubechie's wavelet.

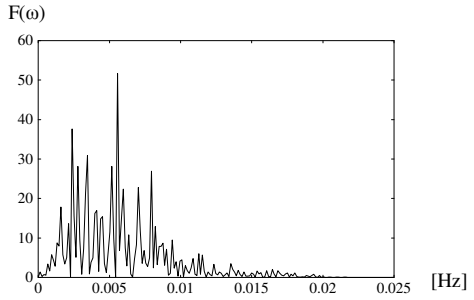

Fig. 6. Fourier spectrum (Path = 415, Row = 319, Jiparana)

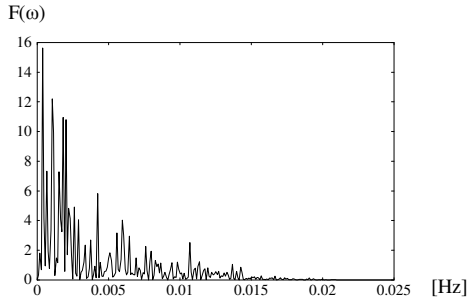

Fig. 7. Fourier spectrum (Path=419, Row=315, Porto Velho)

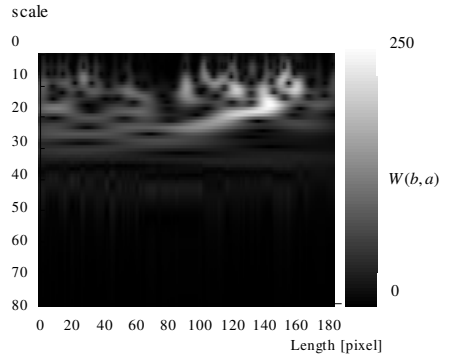

Fig. 8. Space-frequency plane
(Path=415, Row=319, Jiparana)

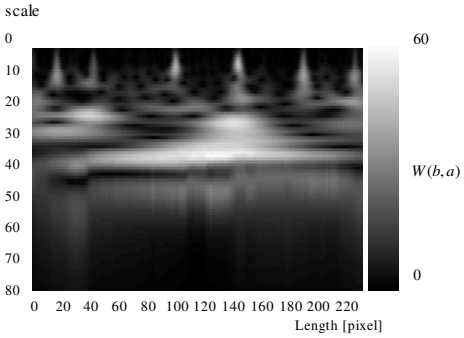

Fig. 9. Space-frequency plane
(Path=414, Row=306, Manaus)

Furthermore, we calculated the averages of every Fourier spectrum, wavelet's scale and level. Thus, we analyzed the meandering of the river shapes, and obtained the average of the spatial frequencies as follows.

$$E = \frac{\sum_{j=1}^{N} j\,\overline{w^{(j)}}}{\sum_{j=1}^{N} \overline{w^{(j)}}} \tag{4}$$

where j = a wavelet's level or scale
$w^{(j)}$ = average of spectral intensity
N = number of the level or scale

Finally, to compare these characteristics with the existing discharge data, we derived each regression equation between the Fourier power spectrum and the discharge, the wavelet's scale and the discharge, the level and the discharge, and the amplitude of the one-dimensional signal and the discharge.
Next, we obtained the macro scaled river characteristics from the drainage map with 1:2,500,000 (Fig. 10). Namely, we analyzed the orders of drainage patterns with the Horton's rule, and we calculated the numbers and the lengths of the branches for each order. Moreover, we obtained the river slopes from DEM. On the other hand, we estimated the river lengths and the drainage area with the Hack's rule. Then, we supposed the invisible rivers in the original images as an order of zero, and estimated the river length, the drainage area, and the discharge of the order of zero with the relationships from the order of one to five (Figs. 11 to 13). Finally, we compared these results with the micro scaled characteristics derived from the SAR images.

3. RESULTS

We could obtain a good correlation between the discharge of the Amazon River branches and the characteristics of the river shapes. The derived regression equations are as follows.

$$\begin{aligned} Q &= 1.17\times10^{6}\,\theta^{-2.35} && (R^2 = 0.787)\\ Q &= 4.95\times10^{8}\,FT + 612 && (R^2 = 0.683)\\ Q &= 1.49\times10^{6}\,CWT - 9690 && (R^2 = 0.819)\\ Q &= 3.65\times10^{5}\,DWT - 9210 && (R^2 = 0.817) \end{aligned} \tag{5}$$

where Q = discharge (m^3/s)
θ = amplitude of the one-dimensional signal (degree)
FT = Fourier power spectrum
CWT = continuous wavelet spectrum
DWT = discrete wavelet spectrum

Furthermore, the river characteristics of an order of zero derived from a macro scaled drainage map were very similar to the narrow open-water channels with less resolution derived from SAR. Then, we showed the average of the numbers and the lengths of the branches for each order from the Madeira

river basin (Table 1), and the estimated numbers, lengths, drainage areas and the average of the discharge of an order of zero (Tabl

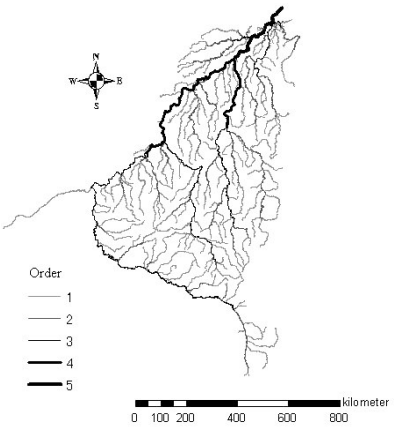

Fig. 10. Drainage map of the Madeira river basin

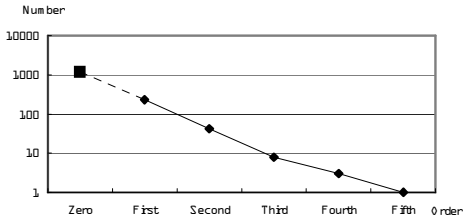

Fig. 11. Number of branches vs. Orders

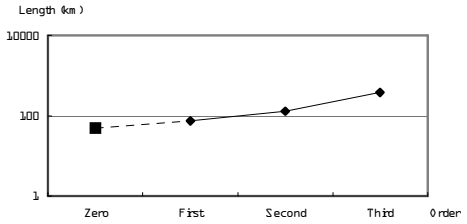

Fig. 12. River lengths vs. Orders

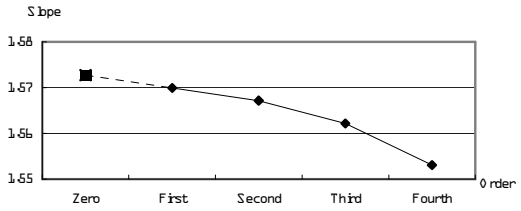

Fig. 13. River slope vs. Orders

Table 1. River characteristics for each order

Order	0 (estimate)	1	2	3	4	5
Number of the branches	1191	227	42	8	3	1
Length of the branches (km)	48.4	82.5	139.6	428.3	507.6	312.4
River slope	1.573	1.570	1.567	1.562	1.553	1.556

Table 2. Estimated characteristics of the order zero and the average of discharge

	Length of the branches (km)	Drainage area (km^2)	Average of the discharge (m^3/s)
Estimate of the order of zero	48.4	632.6	13.5
Invisible river characteristics estimated from SAR	31.5	628.0	13.4

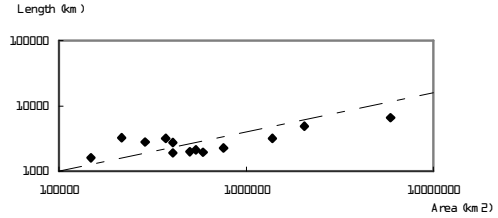

Fig. 14. Lengths vs. Areas

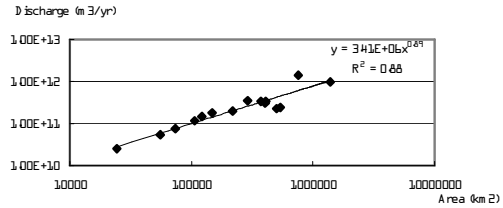

Fig. 15. Discharges vs. Areas

4. CONCLUSIONS

We analyzed the JERS-1/SAR images about 12 scenes from 1993 to 1997 in the Amazon, and found out the characteristics of the river shapes with the river geomorphology correlated the discharge well. Namely, as a result of the Fourier and wavelet analyses, the more discharge had the less spatial frequencies, while the less discharge had the higher spatial frequencies. In particular, we found that the continuous wavelet analysis was the best method to estimate the river discharge. Moreover, by the river geomorphology or Hack's and Horton's rules with the macro scaled drainage map, we could estimate the river characteristics of the order of zero, and they almost corresponded with the invisible river characteristics estimated from SAR images. However, for the reason the characteristics were averaged for each order, the precision had some of error. Therefore, we could obtain the difference between some rivers, but a very small change such as a seasonal change was hard to be derived. In the future, we will analyse and estimate the seasonal change of its discharge with the precipitation data and brightness of the river. Accordingly, by the analysis of the river characteristics, we could estimate the discharge of the narrow branches in the Amazon basin, and monitor the water budget and soil runoff.

References

Takako Sakurai-Amano, Joji Iisaka, and Mikio Takagi, 2000. Detection of narrow open-water channels from JERS-1 SAR images of Amazon forests, *Proc. of SPIE's Second International Asia-Pacific Symposium on Remote Sensing of the Atmosphere, Environment, and Space*, Sendai, Japan, pp.120-130.

Takako Sakurai-Amano, *et al.*, 2001. A year change and monthly division precipitation of a river in the Amazon forest, *Soc. of Photogrammetry and Remote Sensing,* Toyama, Japan.

Shigemi Takagi, 1974. *River Morphology*, Kyoritsu publication.